

Microbial dynamics in the marine ecosystem model ERSEM II with decoupled carbon assimilation and nutrient uptake

J.G. Baretta-Bekker^{a,*}, J.W. Baretta^a, W. Ebenhöb^b

^a Ecological Modelling Centre, Joint Department of Danish Hydraulic Institute and VKI, Agern Allé 5, DK-2970, Hørsholm, Denmark

^b Carl von Ossietzky Universität, Postfach 2503, D-26111, Oldenburg, Germany

Received 28 August 1997; accepted 9 October 1997

Abstract

A description of the improvements in the microbial complex of the dynamical simulation model ERSEM is given and the results for a 130-box setup of the North Sea are discussed. The improvements affecting the microbial food web are the decoupling of the carbon assimilation from the nutrient uptake dynamics in the phytoplankton groups and the incorporation of nutrient uptake dynamics in the bacterioplankton. Simulation results of ERSEM II are presented and discussed in comparison with those of ERSEM I and validation data. Based on model results and emergent properties of the system it was possible to conclude that ERSEM II is able to model the full range of food webs from a system dominated by the microbial loop in the relatively oligotrophic offshore areas to a system dominated by the omnivorous food web in the eutrophic continental coastal area. © 1997 Elsevier Science B.V. All rights reserved.

Keywords: microbial food web; luxury uptake; nutrient uptake; nutrient cycles; ecosystem model; ERSEM

1. Introduction

The traditional view that the herbivorous food web is the dominant form in most, if not all hydrodynamic regimes in marine systems, is now seen as simplistic. The microbial food web is now, 14 years since Azam et al. (1983) first proposed the existence of a 'microbial loop', generally recognised as an important, if not central, component of aquatic systems. It is always present and may be the dominant component in oligotrophic conditions, but relatively unimportant under nutrient-pulse conditions.

Legendre and Rassoulzadegan (1995) make a strong case for the existence of a continuum in

types of food webs, ranging from a dominance of the microbial loop under very oligotrophic conditions to a herbivorous food web in upwelling and other nutrient-pulse situations. Important mechanisms involved in determining which type of food web prevails include the competition between phytoplankton and bacterioplankton for inorganic nutrients and the magnitude of the dissolved organic nutrient pools (both DON and DOP) relative to the magnitude of the DOC pool, which determines whether the bacterioplankton are net nutrient producers or consumers. Another aspect is that large phytoplankton are preferentially grazed by herbivorous zooplankton which transfer nutrients to the dissolved organic pools through both sloppy feeding (Roy et al., 1989) and rapid leaching of faecal pellets (Jumars et al., 1989) and regenerate inorganic nutrients through ex-

* Corresponding author. Tel.: +45 4517 9144; Fax: +45 4576 2567; E-mail: hbb@vki.dk

cretion, especially ammonium and urea. This creates favourable conditions for rapid growth of bacterioplankton and their grazers, enhancing the regeneration and retention of nutrients in the euphotic zone. The shift from the oxidised form of nitrogen, nitrate, to the reduced form, ammonia, is thought to favour the production of small phytoplankton (Riegman et al., 1993).

In situations where all macronutrients are non-limiting, e.g. in upwelling areas and in late winter at higher latitudes, and where grazing pressure on the net phytoplankton is low, a diatom bloom occurs as soon as the surface mixed layer shallows sufficiently (Sverdrup, 1953; Ruardij et al., 1997; Ebenhöf et al., 1997). In the North Sea it is preceded by a small bloom of picoplankton (Riegman et al., 1993) which is quickly suppressed by their ever-present grazers, heterotrophic nanoflagellates and ciliates, that keep the biomass of the bacterioplankton and picoplankton at a relatively constant level (Legendre and Rassoulzadegan, 1995). In the absence of significant grazing losses, a large fraction of the produced biomass sinks to the sediment (Smetacek et al., 1978), usually (depending on the local depth) removing the incorporated nutrients from the euphotic zone. In cases where Si-depletion induces the sinking of the diatom bloom, this is followed by a nanoplankton bloom, with the food web rapidly shifting to what Legendre and Rassoulzadegan (1995) call a multivorous food web, with a high degree of retention and recycling of the remaining nutrients in the euphotic zone. In areas with a more or less concurrent depletion of N, P and Si, the post-bloom food web tends to be even more dominated by the microbial components, unless or until wind-driven mixing events bring regenerated nutrients into the euphotic zone.

Sterner et al. (1995) emphasised the need for a combined model, which could represent the extremes of the food web spectrum, the classical and the microbial food web, but a model representing the whole continuum of Legendre and Rassoulzadegan (1995) would be more realistic. Such a model must then contain the mechanisms, that determine the possible time-varying place of a system in this continuum.

With the European Regional Seas Ecosystem Model version 5.2 a first attempt was made to develop such a model (Baretta et al., 1995; Baretta-Bekker et al., 1995). However, not all the necessary

mechanisms were incorporated in that version of the model. Bacterioplankton was unable to take up inorganic nutrients and the nutrient and carbon uptake dynamics in the phytoplankton groups were coupled, which implied that the C : N : P ratios of the dissolved organic matter, produced by the phytoplankton, were fixed. Consequently, bacterioplankton always was substrate-limited as the excretion products of the phytoplankton always contained sufficient organic nutrients to meet the nutrient requirements of the bacterioplankton.

The main newly incorporated mechanisms that play a role in the functioning of the microbial food web are the ability of bacteria to take up inorganic nutrients and thus to compete with phytoplankton for inorganic nutrients, and the decoupling of carbon and nutrient dynamics in the phytoplankton groups (Droop, 1973, 1974; Nyholm, 1977), allowing the excretion of nutrient-poor dissolved organic matter in the form of carbohydrates.

The aim of this paper is to describe the new mechanisms in the microbial complex as incorporated in version 11 of ERSEM, called ERSEM II in comparison to version 5.2, called ERSEM I, and to discuss the effects on simulated system behaviour.

2. The model domain

The European Regional Seas Ecosystem Model was designed as a generic model of temperate aquatic ecosystem function by confining site-dependent aspects as latitude, depth, irradiance and transparency to the physical submodel. After having been implemented for the whole North Sea, ERSEM has also been implemented in other regional seas, in subregions of the North Sea (Allen, 1997; Lenhart et al., 1997) and in specific locations in the North Sea (Ruardij et al., 1997) or in mesocosms (Baretta-Bekker et al., 1994, 1998).

In all those different models the formulation of the biogeochemical processes defining biological dynamics is identical, except for some of the parameter values. The differences in system behaviour in the various implementations are a consequence of the site-specific and situation-specific advective and diffusive transport exchanges, forcing functions and boundary conditions.

Two different setups for the North Sea are dis-

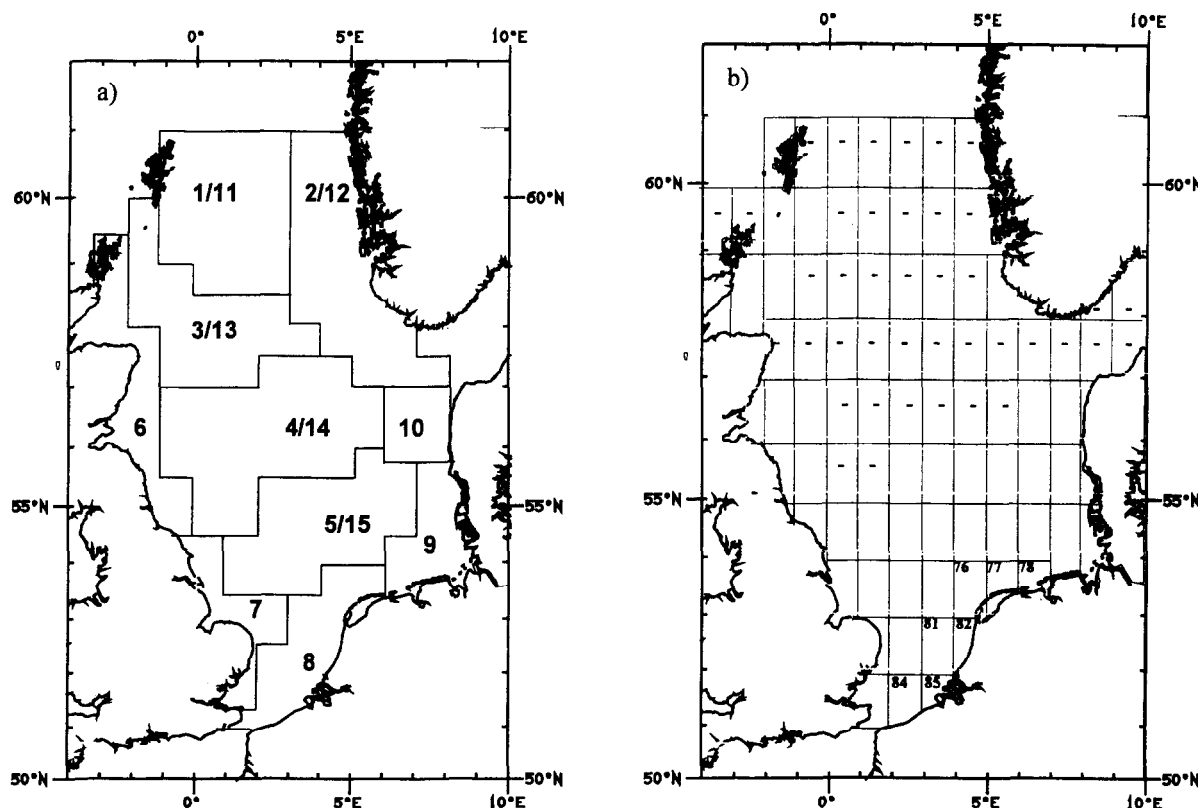


Fig. 1. ERSEM box structure in the 15-box version ND15 and in the 130-box version ND130. (a) The 15-box version has 10 surface boxes, numbered from 1 to 10 and 5 deep boxes with the numbers 11 to 15. (b) The 130-box version has 85 surface boxes, the stratified boxes are indicated with -. The numbered boxes refer to Fig. 9.

cussed in this paper (Fig. 1): (1) ND15, as used during the ERSEM-I project, where the model domain was divided into 15 boxes; and (2) ND130, the standard setup for ERSEM II, which is a spatial setup with 130 boxes. To make a comparison possible between ERSEM I/ND15 and ERSEM II/ND130, the results of ND130 can be aggregated to the 15-box setup.

3. The new features in ERSEM II, affecting microbial food web dynamics

As described in Baretta-Bekker et al. (1995) ERSEM simulates the carbon, nitrogen, phosphorus and silicon cycles in the pelagic and the benthic system. The biological functional groups involved in the microbial food web can be divided into three groups, i.e. the primary producers, the consumers and the decomposers. The availability of inorganic and organic

nutrients which is affected by the activity of these biological groups, plays a key role in system function. The primary producers as modelled in ERSEM I, have been described by Varela et al. (1995), while Baretta-Bekker et al. (1995) gave a description of microzooplankton and bacteria in that version.

In ERSEM I the primary producers were divided into the functional groups autotrophic flagellates (2–20 μm) and diatoms (20–200 μm). In ERSEM II two phytoplankton groups have been added, i.e. picoalgae (0.2–2 μm) and dinoflagellates (20–200 μm). The picoalgae have been included in the light of recent information on their role in the microbial food web in the North Sea (Riegman et al., 1993). The differences between diatoms and dinoflagellates in the model are that the diatoms are dependent on silicate and that the dinoflagellates in contrast to diatoms are not grazed and that they have a lower maximal specific assimilation rate than the diatoms. Other

changes in ERSEM II in comparison to ERSEM I are to be found in the light dependence of the primary producers, as described in Ebenhöf et al. (1997) and in the decoupling of the carbon dynamics from the nutrient dynamics in combination with the ability for luxury uptake of nutrients, as described in the next section.

The model formulation of the microbial consumers, consisting of microzooplankton and heterotrophic nanoflagellates was modified slightly, as described in Baretta-Bekker et al. (1998).

In ERSEM II bacteria are able to take up inorganic nutrients, and do not depend only on the nutrients in the organic matter as in ERSEM I.

4. Detailed description of the decoupling of carbon and nutrient dynamics and of the luxury uptake in the primary producers

In this section, in describing the processes affecting the carbon and nutrient dynamics in the primary producers, the following conventions are used:

- The descriptions are valid for all phytoplankton groups, unless indicated differently. P denotes phytoplankton biomass.
- Instead of daily rates of change, specific rates are used, i.e. the daily rates of change per unit biomass. To calculate the rates of change the specific rates of change have to be multiplied by the actual biomass.
- The name of the specific rate denotes the process, while the lower index denotes the biomass component (c, n, p and s for C, N, P and Si). Thus the phytoplankton biomass in carbon is denoted by P_c and those in the nutrients in P_n , P_p and P_s . An upper index may have been used for other information. In the parameters the process is indicated by the upper index.

In Table 1 the phytoplankton parameters are given. In general the parameters are partly derived from model sensitivity analyses of mesocosm experiments (Baretta-Bekker et al., 1994, 1998) partly from earlier versions of this model concept (Baretta and Ruardij, 1988; Baretta et al., 1995). Last but not least, many parameter values are just educated guesses. The uncertainty as to the true value of these parameters is not as dramatically detrimental to the quality of the model results as one would think.

Ebenhöh et al. (1995) have shown that the dependence of model behaviour on most of the parameter values is weak, due to the complexity of the model which enables it to behave coherently. Modification of a single process by changing a parameter value thus is compensated for by a collective reaction by all other processes.

4.1. The variable intracellular nutrient quota

Because, according to Droop (1973), the growth rate of a phytoplankton population depends on the internal nutrient concentration, the intracellular concentrations of nitrogen and phosphorus in the primary producers are calculated.

Three reference values, relevant for the actual varying nutrient/carbon quota are distinguished. The first value is the minimum value [$x_n^{\min} = (N/C)_{\min}$] the nutrient/carbon ratio can take, corresponding to the nutrient content of the structural parts of the cell. The second value is the Redfield ratio [$x_n^R = (N/C)_{\text{Redfield}}$], which is the average stoichiometric ratio of C:N:P in phytoplankton. The last value specifies the maximum quota [$x_n^{\max} = (N/C)_{\max}$], which corresponds to the storage capacity of the primary producer. The actual values (twice the Redfield ratio as the upper limit and half the Redfield ratio as the lower limit) correspond to the range as given by Sommer (1994).

In the concept used here the Redfield ratio is the threshold value between a nutrient limiting and a non-limiting situation. If one of the actual nutrient/carbon quotas falls below the Redfield value incipient nutrient limitation occurs and loss terms due to excretion and lysis begin to increase.

Depending on the actual (realised) quota x_n and x_p a dimensionless factor e_{np} , with a value between 0 and 1, is defined, describing the intracellular nutrient pool status ($= 1$, if the nutrient/carbon ratio has the Redfield value or higher; $= 0$, if the ratio has the minimum value and the intracellular storage is empty):

$$e_{np} = \min(e_n, e_p), \text{ with}$$

$$e_n = \text{ramp}(0, (x_n - x_n^{\min}) / (x_n^R - x_n^{\min}), 1) \text{ and}$$

$$e_p = \text{ramp}(0, (x_p - x_p^{\min}) / (x_p^R - x_p^{\min}), 1)$$

$$\text{with } \text{ramp}(a, x, b) = \min(b, \max(a, x))$$

Table 1
Parameters as used in the ERSEM-II primary production module

Name	Unit	Meaning	Values
r_{ass}	d^{-1}	maximal assimilation rate	2.5, 2.7, 4.0, 1.5
r_{bas}	d^{-1}	basal respiration	0.15, 0.10
q^{ex}	–	exudation under nutrient stress	0.05, 0.20, 0.20, 0.05
q^{res}	–	respired fraction of production	0.10, 0.25
r_{lys}	d^{-1}	minimal lysis rate	0.05
$r_{\text{dens}}^{\text{lys}}$	d^{-1}	density-dependent mortality rate at 100 mg C m^{-3}	0, 0, 0, 0.01
sed^{min}	m d^{-1}	minimal sedimentation rate	0
sed^{str}	m d^{-1}	nutrient stress sedimentation rate	5.0, 0, 0, 5.0
$e_{\text{np}}^{\text{sed}}$	–	nutrient stress threshold	0.70, 0.75
r_{up}	d^{-1}	maximal rate of storage filling	1
r^{s}	d^{-1}	release rate of excess silicate	1
q^{NO_3}	$(\text{mg C})^{-1} \text{ d}^{-1}$	NO_3 uptake rate (affinity)	0.0025
q^{NH_4}	$(\text{mg C})^{-1} \text{ d}^{-1}$	NH_4 uptake rate (affinity)	0.0025, 0.0025, 0, 0.0025
q^{PO_4}	mg C d^{-1}	PO_4 uptake rate	0.0025
K_{s}	mmol Si m^{-3}	silicate uptake Michaelis constant	0.3
x_{n}^{R}	$\text{mmol N (mg C)}^{-1}$	Redfield N : C ratio	0.01261
$x_{\text{n}}^{\text{max}}$	$\text{mmol N (mg C)}^{-1}$	maximal N : C ratio	$2x_{\text{n}}^{\text{R}}$
$x_{\text{n}}^{\text{min}}$	$\text{mmol N (mg C)}^{-1}$	minimal N : C ratio	$0.55x_{\text{n}}^{\text{R}}$
x_{p}^{R}	$\text{mmol P (mg C)}^{-1}$	Redfield P : C ratio	0.000786
$x_{\text{p}}^{\text{max}}$	$\text{mmol P (mg C)}^{-1}$	maximal P : C ratio	$2x_{\text{p}}^{\text{R}}$
$x_{\text{p}}^{\text{min}}$	$\text{mmol P (mg C)}^{-1}$	minimal P : C ratio	$0.55x_{\text{p}}^{\text{R}}$
x_{s}^{R}	$\text{mmol Si (mg C)}^{-1}$	standard Si : C ratio	0.03
pafr		photosynthetic active fraction	0.5
D_{a}	m	adaptation depth	10
$I_{\text{opt}}^{\text{min}}$	W m^{-2}	minimum for optimal light	4
$I_{\text{opt}}^{\text{max}}$	W m^{-2}	maximum for optimal light	80
η	d^{-1}	light adaptation rate	0.25
Q_{10}	–	Q_{10} -value	2.0

A row of four given values corresponds to the four functional groups of primary producers: diatoms, autotrophic flagellates, picoalgae, dinoflagellates, two values to diatoms and others. If only one value is provided, it is valid for all groups.

It is obvious that instead of the ramp functions for e_{n} and e_{p} and instead of the composition of both factors in the form of a minimum value (Liebig) other formulations could have been selected. A more general formulation is the superposition between the minimum and the product:

$$e_{\text{np}} = \beta \min(e_{\text{n}}, e_{\text{p}}) + (1 - \beta) \times e_{\text{n}} \times e_{\text{p}}$$

$$\text{with } 0 \leq \beta \leq 2$$

The formulation has to fulfil the conditions:

$$e_{\text{np}} = e_{\text{n}} \text{ if } e_{\text{p}} = 1$$

and

$$e_{\text{np}} = e_{\text{p}} \text{ if } e_{\text{n}} = 1$$

The factor e_{np} describing the intracellular nutrient status defines all the loss factors due to nutrient

shortage. It is assumed that the loss terms increase with $(1 - e_{\text{np}})$ to a maximal value if $e_{\text{np}} = 0$. In the case of diatoms an additional factor, e_{s} , has to be defined which describes the external silicate limitation (see Section 4.3).

4.2. The carbon dynamics

Assimilation, excretion and respiration concern only the carbon component of the biomass. The rates of these processes are controlled by the regulation factors e_{I} for the light limitation, e_{T} for the temperature dependence, e_{np} for the combined N- and P-limitations (see Section 4.1) and, in the case of diatoms, e_{s} for the Si-limitation (see Section 4.3).

All these factors are dimensionless. The temperature dependence $e_{\text{T}} = Q_{10}^{\text{temp}/10^\circ - 1}$ has a value 1 for

the reference temperature, 10°C, and for all other temperatures a value determined by the value of Q_{10} . All other factors have values 1 under non-limiting conditions and approach 0 under strongly limiting conditions. With these factors the specific rate ass for the assimilation process can be formulated:

$$\text{ass} = r^{\text{ass}} \times e_T \times e_I \times (e_s)$$

Here the parameter r^{ass} (d^{-1}) is the maximum specific daily assimilation rate at 10°C.

The potential assimilation rate is not dependent on a nutrient limitation due to intracellular N- and P-shortage, nor on the external nutrient concentrations. The idea is that in the case of intracellular nutrient shortage not all the assimilation products can be further processed by the cell into proteins and nucleotides. The unutilisable assimilation products are excreted as excretion products (DOC). The excreted fraction of the assimilation, exu , is modelled as the sum of an activity excretion ($q^{\text{ex}} \times \text{ass}$) and a nutrient-stress-dependent excretion which is proportional to $(1 - e_{\text{np}})$:

$$\text{exu} = \text{ass} \times (q^{\text{ex}} + (1 - q^{\text{ex}}) \times (1 - e_{\text{np}}))$$

The activity and nutrient-stress excretion are linked together. The factor q^{ex} is dimensionless and represents the fraction of ass which is excreted under nutrient-rich conditions (activity excretion is equal to the minimal excretion). Without nutrient limitation ($e_{\text{np}} = 1$) the second part of the equation becomes 0. With $e_{\text{np}} = 0$ in the case of total limitation, the total term becomes equal to ass, which implies that all the assimilation products are converted to DOC and no biomass growth occurs.

The production remaining after subtraction of the excretion is the incorporated primary production ass^{inc} :

$$\text{ass}^{\text{inc}} = \text{ass} - \text{exu}$$

By further subtraction of respiratory losses the net primary production ass^{net} is attained. Respiration, res , in the model consists of basal temperature-dependent respiration $r^{\text{bas}} e_T$ and activity respiration which is a fraction, q^{res} , of ass^{inc} :

$$\text{res} = r^{\text{bas}} e_T + q^{\text{res}} \text{ass}^{\text{inc}}$$

$$\text{ass}^{\text{net}} = \text{ass}^{\text{inc}} - \text{res}$$

The basal respiration $r^{\text{bas}} e_T$ in the model is independent of the uptake, acting only on the biomass.

Due to the basal respiration net primary production may become negative if the light or the nutrient limitations are severe.

Other loss terms include grazing, lysis and sinking. For the description of grazing by microzooplankton and heterotrophic flagellates see Baretta-Bekker et al. (1995) and for grazing by mesozooplankton see Broekhuizen et al. (1995). Lysis is assumed to be enhanced in nutrient-limiting situations, in other words if e_{np} has a low value. Lysis in the model represents non-resolved mortality processes. There may be mechanical causes, viruses, bacteria and yeasts. It is assumed that the average lysis rate increases with nutrient stress. The specific lysis rate is formulated as:

$$\text{lys} = r^{\text{lys}} (1/(e_{\text{np}} + 0.1))$$

r^{lys} is the specific background lysis rate in nutrient-replete situations. No temperature dependence is assumed here. However, having e.g. viruses in mind, this process may also be density dependent. In that case another term is added to lys , with $r_{\text{dens}}^{\text{lys}}$ as the density-dependent mortality rate at a density P_c of 100 mg C m^{-3} :

$$\text{lys} = r^{\text{lys}} \times (1/(e_{\text{np}} + 0.1)) + r_{\text{dens}}^{\text{lys}} \times (P_c/100)$$

The lysis products are partly particulate and partly dissolved. The subdivision for the carbon component of the biomass is defined by a calculated fraction q^{POM} for the part going to particulate organic carbon. This fraction is dependent on the actual and the minimal intracellular nutrient quota for N and P, according to the following equation:

$$q^{\text{POM}} = \min(x_p \min/x_p, x_n^{\text{min}}/x_n)$$

The effect of this equation is that the nutrients in the structural parts of the cell is going to particulate organic carbon when the cell falls apart. The constituents of the cytoplasm are taken to be easily degradable, as well as dissolved, and are added to the dissolved organic pool.

The sedimentation rate is formulated as:

$$\text{sed} = \text{sed}^{\text{str}} \times \max(0, e_{\text{np}}^{\text{sed}} - e_{\text{snp}}) + \text{sed}^{\text{min}}$$

where sed^{str} is the sinking velocity in m d^{-1} under total nutrient limitation, $e_{\text{np}}^{\text{sed}}$ is the nutrient limitation

Table 2

Specific rates determining the carbon dynamics in ERSEM I in comparison with ERSEM II

Specific rate	ERSEM I dependent on	ERSEM II dependent on
Max. assimilation	r^{ass} temperature light external nutrient concentration	r^{ass} temperature light (external Si concentration)
Gross uptake	max. assimilation external nutrient concentration	max. assimilation total excretion and lysis
Lysis, nutrient stress	max. assimilation external nutrient concentration r^{lys}	internal nutrient pool r^{lys} (external Si concentration)
Excretion, nutrient stress	–	max. assimilation internal nutrient pool q^{ex}
Excretion, activity	max. assimilation q^{ex} external nutrient concentrations	max. assimilation q^{ex}
Respiration, basal	temperature r^{bas}	temperature r^{bas}
Respiration, activity	fractional day length incorporated assimilation q^{res} external nutrient concentrations	incorporated assimilation q^{res}
Respiration, nutrient stress	incorporated assimilation q^{str} external nutrient concentrations	–

For explanation of the parameters see Table 1. The bold-printed terms indicate the nutrient limitations. All terms with Si refer to diatoms only.

value below which increased sedimentation occurs, $e_{snp} = \min(e_s, e_{np})$ and sed^{min} is the background sedimentation, which in the model is set on 0. This formulation is basically the same as that described by Varela et al. (1995), except that now the internal nutrient limitation for nitrogen and phosphorus is taken into account, instead of the external nutrient concentrations.

To summarise the differences between ERSEM I and ERSEM II the rates and their dependencies are given in Table 2.

4.3. Nutrient dynamics

4.3.1. Nitrate and phosphate

Nutrient uptake is dependent on the external concentrations of NO_3 , NH_4 , PO_4 and on the degree to which the storage capacity is filled. In the model, the potential nutrient uptake is calculated in dependence of the carbon uptake and the internal nutrient storage

capacity, but also on the affinity of the phytoplankton group for a nutrient and the external nutrient concentration.

Taking the uptake of phosphorus as the simplest example, as only the uptake of orthophosphate has to be considered, the amount of phosphorus the phytoplankton group attempts to take up is the sum of the amount to form new biomass plus the amount to replenish its intracellular storage:

$$up_p^{int} = \underset{\text{growth}}{ass^{net} \times x_p^{max}} + \underset{\text{storage}}{(x_p^{max} - x_p) \times r^{up}}$$

where x_p^{max} is the maximal P/C ratio and r^{up} is the maximal rate of storage filling.

The amount of phosphorus the phytoplankton group can take up at the actual external concentration of PO_4 is defined as follows:

$$up_p^{ext} = q^{PO_4} \times PO_4$$

where q^{PO_4} ($\text{mg C}^{-1} \text{d}^{-1}$) is the affinity of the P-group for PO_4 . The realised uptake is the minimum of the two rates:

$$\text{up}_p = \min(\text{up}_p^{\text{ext}}, \text{up}_p^{\text{int}})$$

In the case of a phosphorus surplus (due to respiration in the absence of primary production) up_p can become negative, and the surplus is excreted as PO_4 .

For nitrogen the treatment is comparable. The first term, up_n^{int} , is calculated in the same way as for phosphorus. In calculating up_n^{ext} there is the complication, that there are two nitrogen sources NH_4 and NO_3 with different preferences defined by the parameters q^{NO_3} and q^{NH_4} for the affinity for NO_3 and NH_4 , respectively:

$$\text{up}_n^{\text{ext}} \text{NO}_3 = q^{\text{NO}_3} \times \text{NO}_3$$

$$\text{up}_n^{\text{ext}} \text{NH}_4 = q^{\text{NH}_4} \times \text{NH}_4$$

$$\text{up}_n^{\text{ext}} = q^{\text{NO}_3} \times \text{NO}_3 + q^{\text{NH}_4} \times \text{NH}_4$$

The realised uptake is the minimum of the two rates:

$$\text{up}_n = \min(\text{up}_n^{\text{ext}}, \text{up}_n^{\text{int}})$$

If up_n is positive, this flux is divided in two parts belonging to the two sources: $(\text{up}_n^{\text{ext}} \text{NO}_3 / \text{up}_n^{\text{ext}}) \times \text{up}_n$ from NO_3 and $(\text{up}_n^{\text{ext}} \text{NH}_4 / \text{up}_n^{\text{ext}}) \times \text{up}_n$ from NH_4 . If this flux becomes negative, because up_n^{int} is negative, excretion only occurs to NH_4 .

4.3.2. Silicate

The only functional group of the primary producers that contains silicate are the diatoms. Silicate dynamics differ from those of nitrate and phosphate in that silicate is not stored internally. The cell quota $x_s R = P_s / P_c$ is essentially equal to the fixed standard value. This is realised by assuming an uptake flux for silicate proportional to the carbon net production:

$$\text{up}_s = \max(0, \text{ass}^{\text{net}} \times x_s^R) - \max(0, x_s - x_s^R) \times r_s^{\text{ex}}$$

In this formulation, the uptake (if $\text{ass}^{\text{net}} > 0$) and the release of excess silicate is separated.

It has to be guaranteed that no silicate uptake occurs if the external SiO_4 -concentration goes to zero. This is achieved by the introduction of a silicate limiting function:

$$e_s = \text{SiO}_4 / (\text{SiO}_4 + K_s)$$

This factor — in contrast to e_n and e_p — contains the external concentration SiO_4 . The maximal specific primary production, ass , contains e_s as a factor (Section 4.2).

5. Results

In presenting the results from the microbial components in the ERSEM model, it has to be kept in mind that the microbial components are part and parcel of the system (as represented by the model) and, as such affect and are affected by the processes that occur in other parts of the system. The results given here show the behaviour of the microbial components in the context of the dynamics of the whole system. To establish whether the changes in the formulation of the phytoplankton/microbial food web part of the model can be considered improvements the time-evolution of the biomass of the functional groups microzooplankton, heterotrophic nanoflagellates and bacterioplankton in some of the boxes are compared with the output of ERSEM I and the sparse observational data, which come from the data base by the British Oceanographic Data Centre (BODC), assembled from data originating from the Natural Environmental Research Council (NERC) North Sea Community Project (Lowry et al., 1992).

In Figs. 3–9 the aggregated results of the spatially resolved ND130 setup of ERSEM II are compared with the results from the ND15 setup of ERSEM I. See Fig. 1 for the box structure of the 15-box version, with the northern boxes 1, 2 and 3, the central boxes 4 and 5, the UK coastal boxes 6 and 7, and the continental coastal boxes 8, 9 and 10.

The time evolution of the microzooplankton in ERSEM II clearly corresponds much closer to the scarce available data than the ERSEM-I results (Fig. 2a), but in box 8 the microzooplankton still is underpredicted during the first half year. The regional differences in microzooplankton abundance are strikingly well reproduced.

The available data of the heterotrophic flagellates biomass distribution do not allow any conclusion to be drawn with respect to whether ERSEM II represents the time and space evolution better than ERSEM I (Fig. 2b).

The bacterioplankton abundance over time (Fig. 2c) has become much more variable with

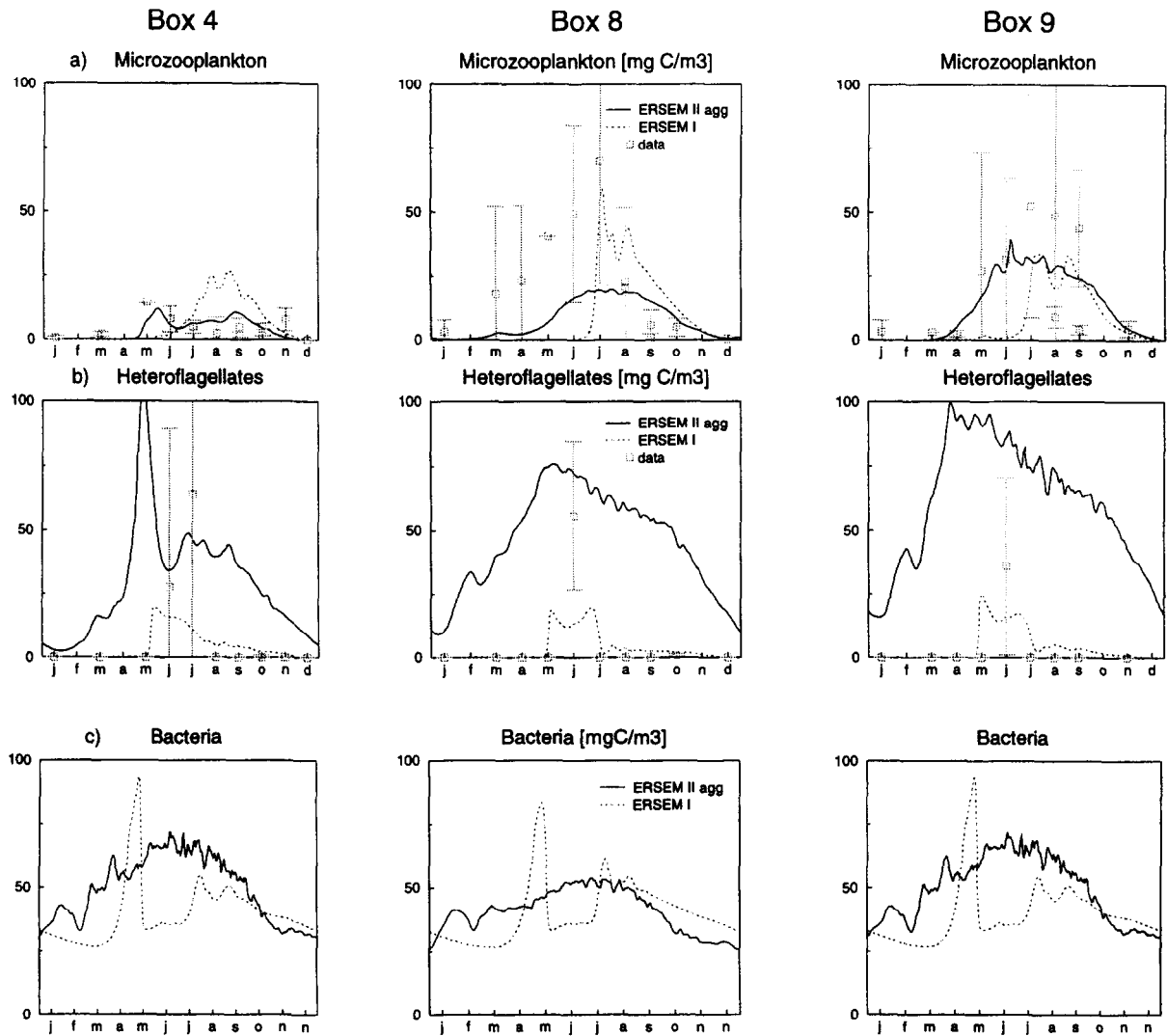


Fig. 2. Results of the standard ERSEM II/ND130 model aggregated to the 15-box setup for the boxes for the state variables (a) microzooplankton, (b) heterotrophic nanoflagellates and (c) bacteria, together with model results of ERSEM I/ND15 and field data from the BODC data base with standard deviations. All biomasses in mg C m^{-3} .

higher frequency variability than in ERSEM I, but the fundamental seasonal biomass evolution follows the primary production curve very closely (Fig. 3). Irradiance influences gross primary production (assimilation) directly, and thereby the production of dissolved organic matter, which is the main substrate for bacteria.

Other results that are of interest are the effects of the improvements in the microbial food web dynamics in ERSEM II on the concentrations of the different nutrients in comparison with the results

of ERSEM I (Fig. 4). The nutrient concentrations in general as reproduced by ERSEM II track the observations during the NERC North Sea survey much better than ERSEM I.

For phosphate (Fig. 4a) the model results of ERSEM II in comparison with the results of ERSEM I indicate lower values in the northern and central boxes with high values in summer which correspond better to observations. The different seasonality in the phosphate data in the various boxes is reproduced very well for box 4, 5 (not shown), 7 (not

Box 1

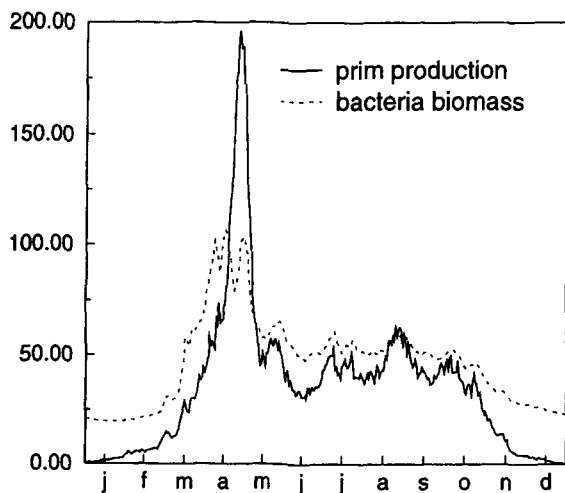


Fig. 3. Results of the standard ERSEM II/ND130 model aggregated to the 15-box setup for box 1 for primary production in $\text{mg C m}^{-3} \text{ d}^{-1}$ and bacterioplankton biomass in mg C m^{-3} .

shown) and 9. However, the observed higher values in autumn are not reproduced by the model.

The observed summer values for nitrate (Fig. 4b) are reproduced accurately, but the start of the decrease of the concentration in late winter/early spring with the modelled decrease in dissolved concentrations does not coincide as well everywhere, as the data indicate a decreasing tendency from January on, most clearly in box 4. However, the rate and timing of almost complete depletion of nitrate in the surface water is generally correct, as is the increase in autumn.

Ammonium (Fig. 4c) shows a fundamental improvement over the results of ERSEM I, there being no obvious seasonality neither in the observations nor in the modelled concentrations. The concentrations now are reproduced quite well in the central and eastern North Sea boxes, but have a tendency of being overpredicted in the coastal boxes.

The spring decrease in silicate concentrations (Fig. 4d) begins earlier, which is in better agreement with the observations. The low summer values now are reproduced almost perfectly, but the observed higher values in autumn in boxes 5 and 7 (not shown) are not reproduced by the model.

Of even more interest are the model results that provide information about the regional differences in the internal structure and functioning of the system and how these vary in time and space. These differences are most clearly apparent in the fluxes of carbon and the nutrients.

Phytoplankton take up nitrogen in the form of ammonia and/or nitrate. Fig. 5 gives the fluxes from ammonia and nitrate to the total phytoplankton, indicating the regional different availability of ammonia and nitrate.

Bacteria in this model version can take up inorganic as well as organic nutrients. For nitrogen it is only the reduced form — NH_4 —, that is taken up by the bacteria in the model. This is a simplification, as bacteria also are able to take up NO_3 , but they prefer the reduced form (Kirchman et al., 1992). Fig. 6 shows when and where the bacteria have a net uptake of nutrients and when and where they mineralise nutrients. For nitrogen this is as follows: going from box 1 (oligotrophic) to box 9 (eutrophic), the net uptake of nitrogen changes to a net mineralisation changing the role of the bacterioplankton from being nitrogen competitors of the phytoplankton to nitrogen suppliers, while the bacteria in the oligotrophic as well as in the eutrophic areas of the North Sea compete for phosphorus with the phytoplankton.

6. Discussion and conclusions

Compared to ERSEM I, ERSEM II is more resolved, not only with regard to the spatial resolution of the model domain with 130 boxes in ERSEM II, versus only 15 in ERSEM I, but also in the formulation of the microbiological processes. The reformulation is based on conclusions from analysing the microbial dynamics in the ERSEM-I model (Baretta-Bekker et al., 1994, 1995). These results indicated that the nutrient dynamics were too simplistic and that it would be necessary to include luxury uptake in the phytoplankton formulation as well as internal nutrient storage, which implies a decoupling of carbon assimilation and nutrient uptake kinetics. The effect of this decoupling as well as the effect of luxury uptake has been discussed in Baretta-Bekker et al. (1998), where the pelagic part of ERSEM II has been used in its zero-dimensional form as a one-box model without transport to simulate mesocosm

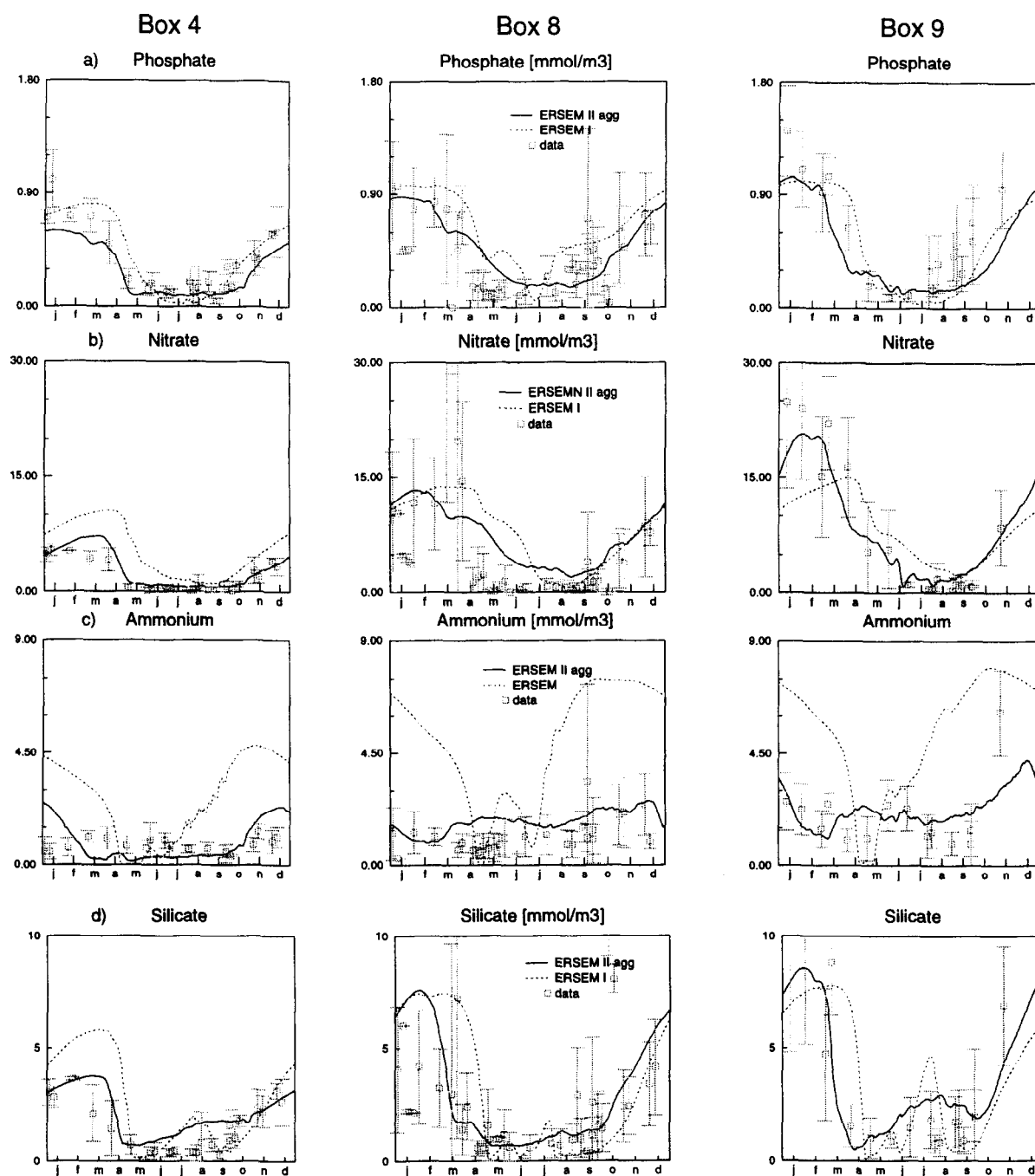


Fig. 4. Results of the standard ERSEM II/ND130 model aggregated to the 15-box setup for the boxes 4, 8 and 9 of the concentrations of the nutrients (a) phosphate, (b) nitrate, (c) ammonium and (d) silicate, in the water together with model results of ERSEM I/ND15 and field data from the BODC data base with standard deviations. All concentrations in mmol m^{-3} .

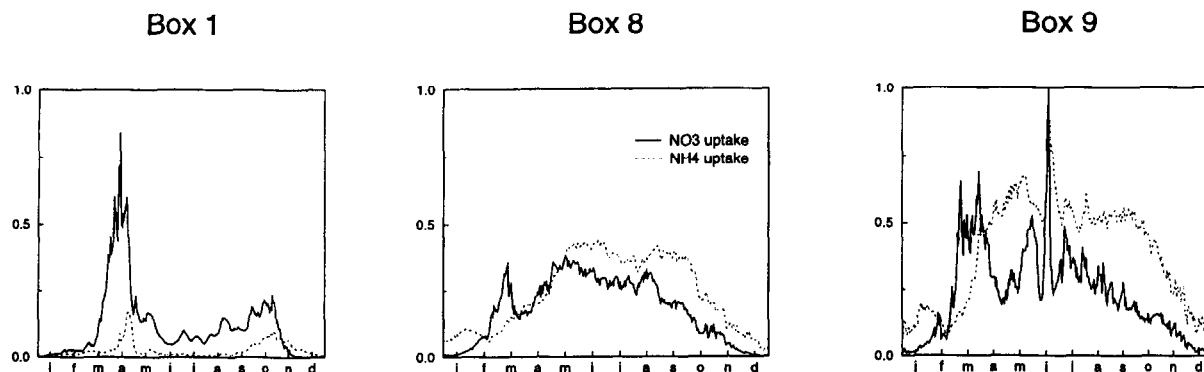


Fig. 5. Results of the standard ERSEM II/ND130 model aggregated to the 15-box setup for nitrate and ammonia uptake by the phytoplankton groups in $\text{mmol N m}^{-3} \text{d}^{-1}$.

experiments. A major conclusion of that study was that luxury uptake has an effect only in situations with poor nutrient availability, while decoupling of carbon assimilation from nutrient uptake has large effects in nutrient-replete situations.

As the differences between ERSEM I and ERSEM II are not confined to the changes in the microbial modules, it is difficult to draw conclu-

sions concerning the changes in the microbial complex from a direct comparison between ERSEM-I results and ERSEM-II results. Nevertheless, a major difference is that carbon assimilation by primary producers was close to zero until the end of February in ERSEM I in all surface boxes, whereas ERSEM II predicts assimilation to continue (at a low level) also during winter (Fig. 7).

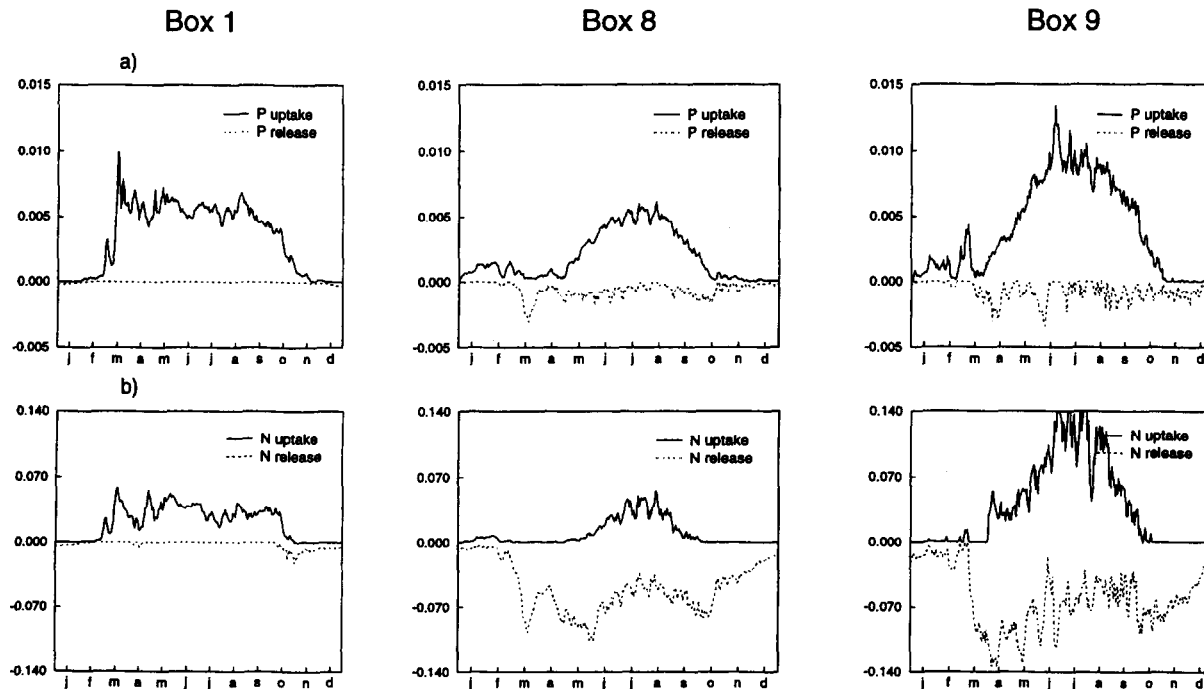


Fig. 6. Results of the standard ERSEM II/ND130 model aggregated to the 15-box setup for nutrient uptake and release by bacteria for the boxes 1, 8 and 9; (a) phosphorus in $\text{mmol P m}^{-3} \text{d}^{-1}$; (b) nitrogen in $\text{mmol N m}^{-3} \text{d}^{-1}$.

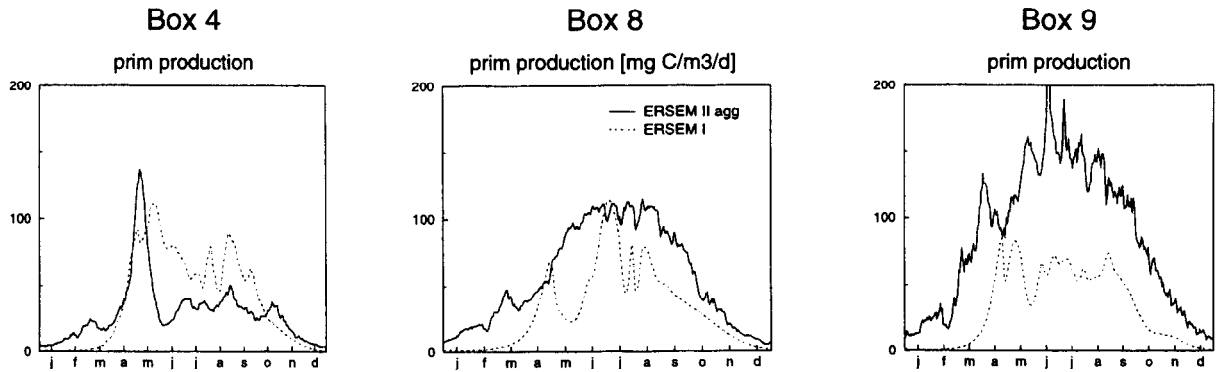


Fig. 7. Results of the standard ERSEM II/ND130 model aggregated to the 15-box setup for the boxes 4, 8 and 9 of the gross primary production ($\text{mg C m}^{-3} \text{ d}^{-1}$) together with model results of ERSEM I/ND15.

This is caused by the higher biological resolution in the primary producers, with picoalgae continuing to have a net production during winter. As a consequence the values of the nutrient turnover times in winter in ERSEM I are much higher than in ERSEM II. The nutrient turnover times are here defined as $t_p = 24\{\text{PO}_4/(\text{up}_p \times P_p)\}$ for phosphorus and as $t_n = 24\{(\text{NO}_3 + \text{NH}_4)/(\text{up}_n \times P_n)\}$ for nitrogen, with up_p and up_n the specific nutrient uptake rates for

phosphorus and nitrogen and PO_4 , NO_3 and NH_4 the concentrations of the nutrients. During summer, the nitrogen and phosphorus turnover times predicted by ERSEM I for the northern North Sea are lower than those predicted by ERSEM II, because ERSEM I draws down the levels of dissolved inorganic nitrogen (DIN) and phosphorus (DIP) in the offshore boxes too far in contrast to ERSEM II (Fig. 4a,b). In the coastal boxes, ERSEM II predicts summer

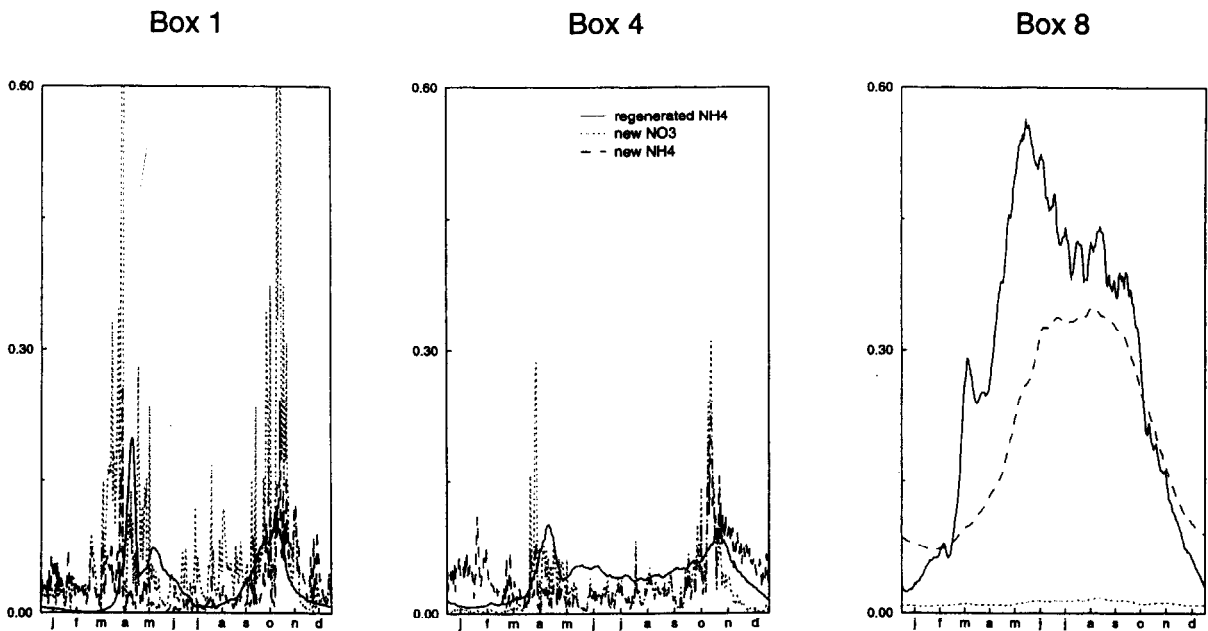


Fig. 8. Results of the standard ERSEM II/ND130 model aggregated to the 15-box setup for the regenerated NH_4 flux, and the diffusive transport fluxes of NH_4 (new NH_4) and NO_3 (new NO_3) in $\text{mmol N m}^{-3} \text{ d}^{-1}$. For the boxes 1 and 4 the diffusive transport flux is across the thermocline from the underlying boxes (11 and 14) and in box 8 directly from the sediment.

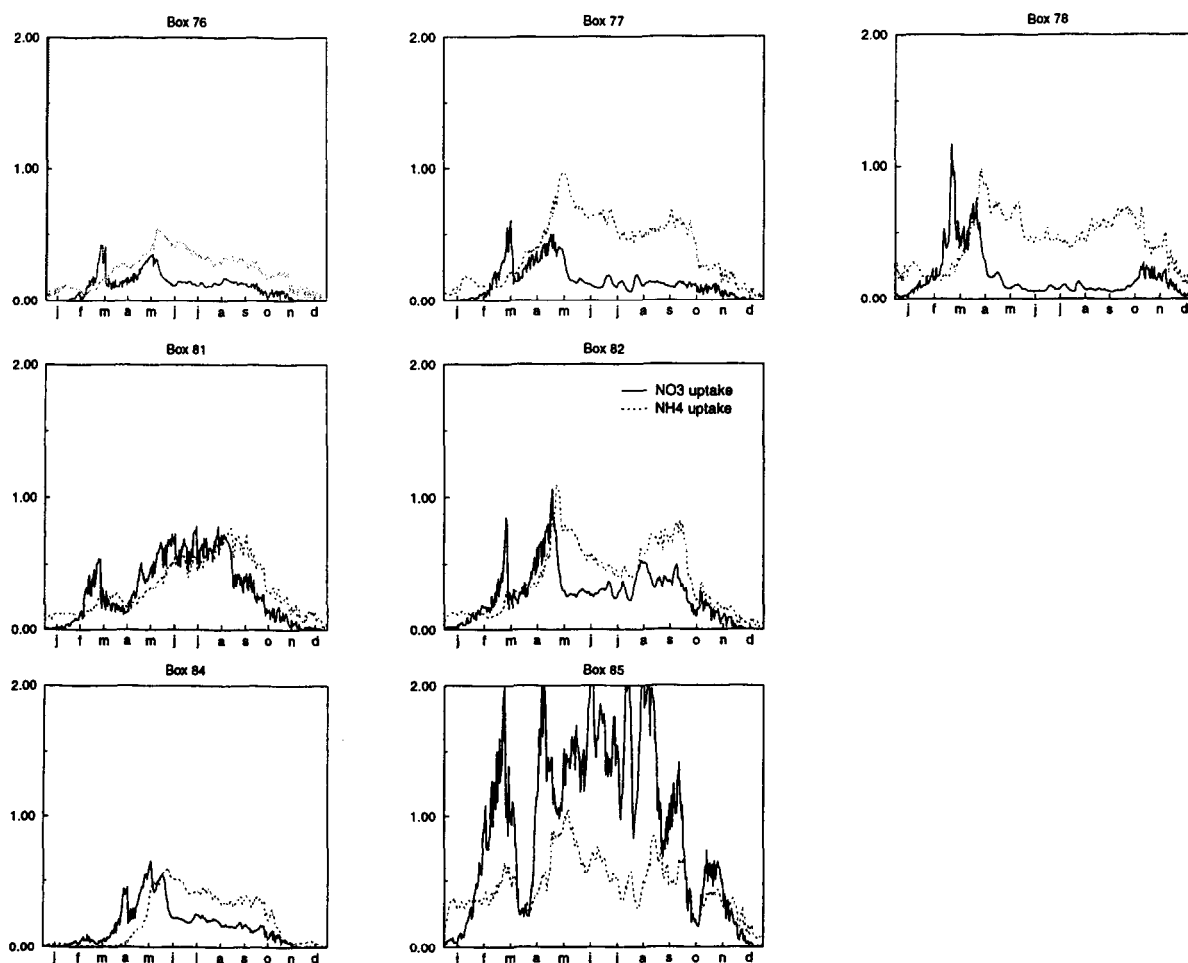


Fig. 9. Results of the standard ERSEM II/ND130 model for the nitrate and ammonia uptake fluxes by the phytoplankton groups in $\text{mmol N m}^{-3} \text{ d}^{-1}$. These boxes comprise box 8 of the ND15 setup (see Fig. 1).

turnover times for nitrogen of 75 to 175 h, with the shortest turnover time in the Danish coastal box (box 10). Predicted phosphorus turnover times lie between 75 and 100 h, which is at the upper end of the range of 1 to 3 days for systems with a normally structured foodweb (Sorokin et al., 1996). ERSEM I predicts far higher turnover times in these boxes, indicating both an overprediction of DIN and/or DIP concentrations and an underprediction of nutrient-uptake fluxes. The N and P turnover times as an indicator of system state thus appear to be more sensitive than DIN and DIP concentrations, because identical nutrient concentrations may and do occur at widely different productivity and mineralisation levels.

In the ERSEM-II formulation defining N-uptake kinetics of the phytoplankton groups, no preference for either NO_3 or NH_4 is assumed. This implies that the relative distribution of NO_3 -uptake versus NH_4 uptake is dependent on the supply flux of NO_3 versus NH_4 , which need not at all be proportional to their relative concentrations as NO_3 is a typical allochthonous supply, based on accumulation and physical transport over larger spatial and temporal scales, whereas NH_4 represents the immediate autochthonous supply via regeneration in the water column at short spatial and temporal scales (Eppey, 1981; Goldman, 1984; Tamminen, 1995).

The model results confirm the conclusions from Tamminen (1995), who found that the relative pro-

portion of new and regenerated production was regulated mainly by the relative supply rates of nitrate through physical transport and of ammonium through mineralisation processes. This conclusion is supported by the model results (Fig. 5) in that in box 1 with a very variable supply of NO_3 in summer from across the thermocline and a low level of remineralisation in the euphotic zone (Fig. 8), nitrate uptake dominates ammonium uptake over the whole year. In the central North Sea (box 4), with higher rates of both NO_3 and NH_4 supply, NH_4 uptake begins to exceed NO_3 uptake as remineralisation increases. In box 8, where the river Rhine enters the North Sea, ammonium uptake dominates the whole year round except during the start of the spring bloom. Interestingly, a further confirmation of supply-side dynamics is given by the spatially better resolved ND130, because within the aggregated box 8, in the region closest to the outflow of the Rhine (small box 85) the rate of supply of NO_3 exceeds the NH_4 supply and as a consequence, NO_3 uptake dominates the whole year (Fig. 9).

Another new aspect in the ERSEM-II model is the production of nutrient-poor exudates of phytoplankton in the form of carbohydrates, which is a direct consequence of the decoupling of the nutrient uptake and carbon assimilation processes. This nutrient-poor substrate can be utilized by bacterioplankton, because of their ability to take up inorganic nutrients. In situations of limited nutrient availability and consequently nutrient-poor carbon substrate supply, bacterioplankton can become a competitor of phytoplankton for nutrients. This mechanism gives rise to regionally very different rates of direct versus indirect transfer of biogenic particulate matter. Direct transfer is defined as the grazing flux directly from primary production to microzooplankton and heterotrophic nanoflagellates, whereas the indirect transfer is defined as the grazing flux from bacterioplankton into microzooplankton and heterotrophic nanoflagellates. These fluxes can also be viewed as the recycling of dissolved organic matter by and in the microbial loop. Note that in this indirect transfer flux also the excretion products of all heterotrophic variables play a role as they supplement the substrate (DOC) which the bacterioplankton utilizes. Division of the direct transfer flux by the indirect transfer flux, results in a dimensionless ratio, which

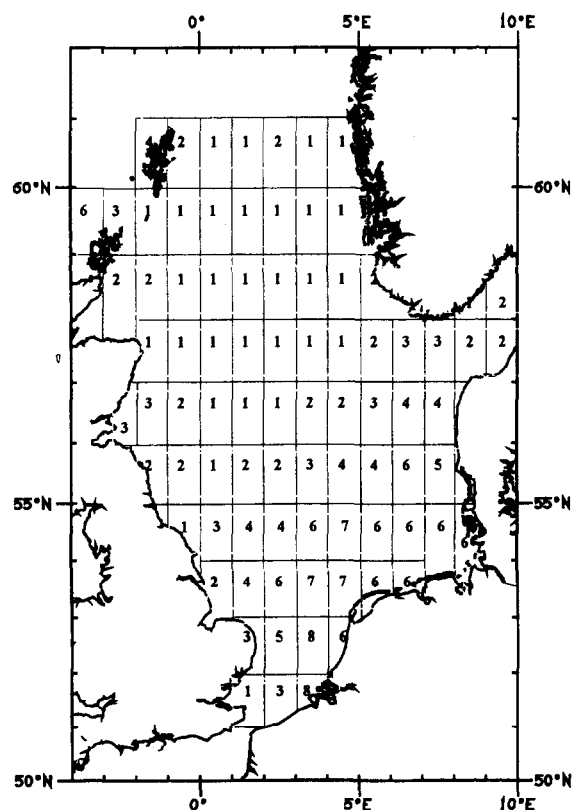


Fig. 10. The ratio of the carbon flux from phytoplankton to the small heterotrophs (microzooplankton plus heterotrophic nanoflagellates) divided by the carbon flux from bacteria to the small heterotrophs for all surface boxes of the 130-box setup, multiplied by ten and rounded.

multiplied by 10 and rounded is given in Fig. 10 for all surface boxes of ND130. There is a clear NW (oligotrophic)–SE (eutrophic) gradient of this ratio, with the direct transfer increasingly larger with increasing nutrient availability and, conversely the indirect flux being up to ten times as large as the direct transfer in the central and northern North sea, underscoring the central role of microbial components in recycling and retaining carbon and nutrients in the euphotic zone.

Using the same approach, but now with the grazing flux from phytoplankton to mesozooplankton as the direct flux (Fig. 11), generally the same regional distribution is seen, with the direct flux to mesozooplankton close to the continental coast being up to six times as large as in the northern central boxes. The much higher values in the boundary boxes are

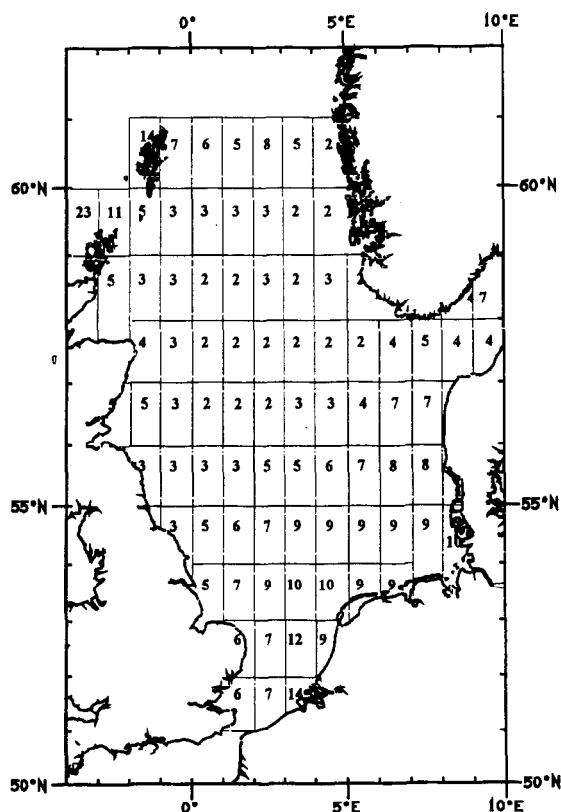


Fig. 11. The ratio of the carbon flux from phytoplankton to mesozooplankton divided by the carbon flux from bacteria to the small heterotrophs (microzooplankton plus heterotrophic nanoflagellates) for all surface boxes of the 130-box setup, multiplied by ten and rounded.

due to explicit boundary conditions for the mesozooplankton. The rationale to use the flux from bacteria to the microzooplankton components instead of the flux from phytoplankton to dissolved organic matter, was to make the recovery of dissolved organic matter into particulate organic matter (i.e. bacterioplankton) explicit, as bacterial production may as well be nutrient-limited as substrate-limited (Thingstad et al., 1993).

The main conclusion from the results presented is that ERSEM II is able to model a continuum of food webs. From the eutrophic coastal zone to the relatively oligotrophic offshore areas there is a gradient from a system dominated by the multivorous web to a system dominated by the microbial loop. For example Fig. 6 shows that bacteria in the aggregated box 1 are taking up nitrogen, which Legendre

and Rassoulzadegan (1995) see as characteristic of a system dominated by the microbial loop. In the large box 8 the mineralisation of nitrogen by bacteria exceeds the uptake, characteristic of a system dominated by the multivorous web, while box 9 according to this characteristic is dominated by the microbial food web. In Figs. 10 and 11 the same gradients can be seen.

As this paper is meant primarily to describe the newly incorporated mechanisms in the microbial complex in ERSEM II, the model analysis made here is not exhaustive. Many interesting and possibly illuminating avenues for computational ecology remain unexplored.

Acknowledgements

We gratefully acknowledge the support from MAST, under contract number MAS2-CT92-0032-C. We thank Piet Ruurdij and Ursula Gaedke for their valuable comments on an earlier version of the manuscript, Cora Kohlmeier and Frank Hamburg for the data-analysis and -display software tool MoViE which allowed us to make sense of complex model results and Paul Turner is gratefully acknowledged for the availability of the graphical package XVGR.

References

- Allen, I., 1997. A modelling study of the ecosystem dynamics of the Humber Plume, UK. *J. Sea Res.* 38, 333–359 (this issue).
- Azam, F., Fenchel, T., Field, J.G., Gray, J.S., Meyer-Reil, L.-A., Thingstad, F., 1983. The ecological role of water-column microbes in the sea. *Mar. Ecol. Prog. Ser.* 10, 257–263.
- Baretta, J.W., Ruurdij, P. (Eds), 1988. Tidal Flat Estuaries. Simulation and Analysis of the Ems Estuary. *Ecological Studies*, Vol. 71. Springer, Berlin, pp. 1–353.
- Baretta, J.W., Ebenhö, W., Ruurdij, P., 1995. The European Regional Seas Ecosystem Model, a complex marine ecosystem model. *Neth. J. Sea Res.* 33, 261–270.
- Baretta-Bekker, J.G., Riemann, B., Baretta, J.W., Rasmussen, E.K., 1994. Testing the microbial loop concept by comparing mesocosm data with results from a dynamical simulation model. *Mar. Ecol. Prog. Ser.* 106, 187–198.
- Baretta-Bekker, J.G., Baretta, J.W., Rasmussen, E.K., 1995. The microbial food web in the European Regional Seas Ecosystem Model. *Neth. J. Sea Res.* 33, 363–379.
- Baretta-Bekker, J.G., Baretta, J.W., Hansen, A.S., Riemann, B., 1998. An improved model of carbon and nutrient dynamics in the microbial food web in marine enclosures. *Aquat.*

- Microbial. Ecol. 14, 91–108.
- Broekhuizen, N., Heath, M.R., Hay, S.J., Gurney, W.S.C., 1995. Modelling the dynamics of the North Sea's mesozooplankton. *Neth. J. Sea Res.* 33, 381–406.
- Droop, M.R., 1973. Some thoughts on nutrient limitation in algae. *J. Phycol.* 9, 264–272.
- Droop, M.R., 1974. The nutrient status of algal cells in continuous culture. *J. Mar. Biol. Ass. UK* 54, 825–855.
- Ebenhöh, W., Kohlmeier, C., Radford, P.J., 1995. The benthic biological submodel in the European Seas Ecosystem Model. *Neth. J. Sea Res.* 33, 423–452.
- Ebenhöh, W., Baretta-Bekker, J.G., Baretta, J.W., 1997. The primary producer module in the marine ecosystem model ERSEM II, with emphasis on the light forcing. *J. Sea Res.* 38, 173–193 (this issue).
- Eppley, R.W., 1981. Autotrophic production of particulate matter. In: Longhurst, A.R. (Ed.), *Analysis of Marine Ecosystems*. Academic Press, London, pp. 343–361.
- Goldman, J.C., 1984. Oceanic nutrient cycles. In: Fasham, M.J.R. (Ed.), *Flows of Energy and Materials in Marine Ecosystems. Theory and Practice*. Plenum Press, New York, pp. 137–170.
- Jumars, P.A., Penry, D.L., Baross, J.A., Perry, M.J., Frost, B.W., 1989. Closing the microbial loop: Dissolved organic carbon pathway to heterotrophic bacteria from incomplete ingestion, digestion and absorption in animals. *Deep-Sea Res.* 36, 483–495.
- Kirchman, D.L., Moss, J., Keil, R.G., 1992. Nitrate uptake by heterotrophic bacteria: Does it change the *f*-ratio?. *Arch. Hydrobiol. Beih.* 37, 129–138.
- Lenhart, H.J., Radach, G., Ruardij, P., 1997. The effects of river input on the ecosystem dynamics in the continental coastal zone of the North Sea using ERSEM. *J. Sea Res.* 38, 249–274 (this issue).
- Legendre, L., Rassoulzadegan, F., 1995. Plankton and nutrient dynamics in marine waters. *Ophelia* 41, 153–172.
- Lowry, R., Cranmer, K., Rickards, L., 1992. North Sea Project CD ROM and User Guide. British Oceanographic Data Centre, Natural Environmental Research Council, Swindon, UK.
- Nyholm, N., 1977. Kinetics of nitrogen-limited algal growth. *Prog. Wat. Technol.* 8, 347–358.
- Riegman, R., Kuipers, B.R., Noordeloos, A.A.M., Witte, H.J., 1993. Size-differential control of phytoplankton and the structure of plankton communities. *Neth. J. Sea Res.* 31, 255–265.
- Roy, S., Harris, R.P., Poulet, S.A., 1989. Inefficient feeding by *Calanus helgolandicus* and *Temora longicornis* on *Coscinodiscus wailesii*: quantitative estimation using chlorophyll-type pigments and effects on dissolved free amino acids. *Mar. Ecol. Prog. Ser.* 52, 145–153.
- Ruardij, P., Van Haren, H., Ridderinkhof, H., 1997. The impact of thermal stratification on phytoplankton and nutrient dynamics in shelf seas: a model study. *J. Sea Res.* 38, 311–331 (this issue).
- Smetacek, V., Von Bröckel, K., Zeitzschel, B., Zenk, W., 1978. Sedimentation of particulate matter during a phytoplankton spring bloom in relation to the hydrographical regime. *Mar. Biol.* 47, 211–226.
- Sommer, U., 1994. *Planktologie*. Springer-Verlag, Berlin, 274 pp.
- Sorokin, Y.I., Dallochio, F., Gelli, F., Pregolato, L., 1996. Phosphorus metabolism in anthropogenically transformed lagoon ecosystems: the Comacchio Lagoons (Ferrara, Italy). *J. Sea Res.* 35, 243–250.
- Sterner, R.W., Chrzanowski, T.H., Elser, J.J., George, N.B., 1995. Sources of nitrogen and phosphorus supporting the growth of bacterio- and phytoplankton in an oligotrophic Canadian shield lake. *Limnol. Oceanogr.* 40, 242–249.
- Sverdrup, H.U., 1953. On conditions for the vernal blooming of phytoplankton. *J. Cons. Int. Explor. Mer* 18, 287–295.
- Tamminen, T., 1995. Nitrate and ammonium depletion rates and preferences during a Baltic spring bloom. *Mar. Ecol. Prog. Ser.* 120, 123–133.
- Thingstad, T.F., Skjoldal, E.F., Bohne, R.A., 1993. Phosphorus cycling and algal–bacterial competition in Sandsfjord, western Norway. *Mar. Ecol. Prog. Ser.* 99, 239–259.
- Varela, R.A., Cruzado, A., Gabaldón, J.E., 1995. Primary production. *Neth. J. Sea Res.* 33, 337–361.